Available online at www.sciencedirect.com
SCIENCE DIRECT®
Journal of Solid State Chemistry 176 (2003) 273–278
JOURNAL OF SOLID STATE CHEMISTRY
http://elsevier.com/locate/jssc

Preparation, crystal structure and electrorheological performance of nano-sized particle materials containing ZrO_2

Fu-Hui Liao,[a] Le Zhang,[a] Jun-Ran Li,[a,*] Gang Xu,[a] Guo-Bao Li,[a] Shao-Hua Zhang,[b] and Song Gao[a]

[a] *State Key Laboratory of Rare Earth Materials Chemistry and Applications, College of Chemistry and Molecular Engineering, Peking University, Beijing 100871, China*
[b] *School of Vehicle and Transmission Engineering, Beijing Institute of Technology, Beijing 100081, China*

Received 15 May 2003; received in revised form 24 July 2003; accepted 2 August 2003

Abstract

A series of nano-sized particle materials containing ZrO_2 was prepared and their compositions were determined by elemental analysis and thermogravimetric analysis (TGA). The effect of particle size and crystal structure type (lattice and space group) on the ER performance of these materials was investigated by X-ray diffraction (XRD) analysis, Raman spectra, the particle size analysis and rheological measurement. Their electrorheological (ER) effects show that the ER activities of the ZrO_2 materials doped with rare earth (RE = Y, La, Ce, Gd, Tb), whose grain sizes were less than that of pure ZrO_2, were lower than that of pure ZrO_2, which belongs to the tetragonal crystal system. The ER activity of Y_2O_3–ZrO_2 is the strongest among all the RE-doped ZrO_2 materials. The ER activity of the tetragonal phase ZrO_2 is higher than that of the monoclinic phase ZrO_2.

Keywords: Rare earth; Crystal structure; Particle size; ER effect

1. Introduction

Electrorheological fluids (ERF) have attracted enormous attention because of their potential usage in devices such as valves, dampers, clutches, brakes, or robotic actuators [1,2]. The mechanism of the ER effect has been intensively discussed in many review articles [2]. A generally accepted concept for the positive ER effect is that the particles form fibrillated chains, which cause an abrupt increase in the rheological parameters. Since the ER effect is induced by an external electric field, the polarization is believed to play an important role; and the particle dielectric property should be dominant in the ER effect. It is well known that the crystal structure, grain size, and composition of the particles, which will influence the physical and chemical natures of a material, are essential to the dielectric and polarization properties of the material. Therefore, it is possible to modify a material's dielectric and polarization properties by adjusting the synthetic procedure such that an ER material having a desired crystal structure, grain size, and composition is produced. The crystal structures of some ER materials have been studied [3–7]. H. Bose and A. Trendler [4] investigated one group of ER fluids containing perovskite type particles. Their results show that these ER fluids obey a polarization mechanism, which is attributed to the local displacement of ions in the crystal structure of the particles. The contribution of conduction to ER activity is low, and the electric properties of these ER fluids are nearly constant. The increase of shear stress with frequency is in accordance with the polarization model. Several authors have reported that adulteration with rare earth compounds can enhance the ER activity of particle materials [6–16]. Zhao Xiao-Ping et al. [13] attributed the improvement of ER effect of doped TiO_2 to the modification of its dielectric and conduction properties, in particular, the increase of dielectric loss or conductivity, which comes with doping with rare earth elements. Furthermore, they consider that the presence of crystalline states, such as lattice distortion, defects, and impurity, may be responsible for the modification of the dielectric and conduction properties of TiO_2. However, up to now no clear relation has been established between the ER activity of a material and

*Corresponding author. Fax: +86-1062751708.
E-mail address: lijunran@pku.edu.cn (J.-R. Li).

0022-4596/$ - see front matter © 2003 Elsevier Inc. All rights reserved.
doi:10.1016/j.jssc.2003.08.007

its crystal structure type. Therefore, it is necessary to research the influence of the crystal structure type of a particle material on its dielectric or conduction properties, and its ER performance.

Nano-sized ER materials were synthesized [17,18]; however, few research works addressed the question of how the size of a nano-sized particle material influences its ER effect [19,20]. The previous research showed a weak ER activity for ZrO_2 [21], but, the effect of the rare earth doping and the structure on the ER activity of ZrO_2 material still are not very clear. In order to obtain a better understanding on the mechanism of the ER effect, we synthesized eight types of nano-sized particle materials containing ZrO_2 in ethanol solution. The effect of the grain size on ER performance, and the relationship between crystal structure type of the particles and their dielectric properties and ER effect were investigated.

2. Experimental

The RE-doped (RE = Y, La, Ce, Gd, Tb) ZrO_2 materials were synthesized by adding aqueous ammonia into ethanol solutions containing $ZrOCl_2$ and $RE(NO_3)_3$ (1: 0.2 molar ratio), followed by washing the hydroxide sedimentations with ethanol, and finally roasting at 400°C for 4 h to decompose the hydroxide sedimentations. Samples 2–6 were thus obtained. The ZrO_2 material (sample 1) without RE was prepared by a procedure similar to the one mentioned above. The preparations of the other two types of materials were as follows: Ethanol solutions of $ZrOCl_2$ were evaporated; the resulting white powders were dried for 6 h at 80°C; and finally the powders were roasted for four hours at 400°C (sample 7) or 600°C (sample 8), respectively.

The compositions of these materials were determined by elemental analyses and TGA (DU PONT 1090B thermal analyzer), showing no water in these materials. The results are listed in Table 1.

The XRD analyses of the materials were performed on a Bruker D8 ADVANCE X-ray diffractometer. The Raman spectra were recorded on a Nicolet Raman 950 spectrometer. The crystal structure types of different particle materials are listed in Table 1.

Various particle materials were dispersed in silicone oil and stirred fully (weight fraction 25%) to make all the ERF samples. The electrorheological experiments were performed using a German Rotary Viscometer (Type HAAKE CV20). The apparatus can work under the given temperature and electrode clearance to measure the anti-shear stress and apparent viscosity of a fluid at various shear states, and it has the function of controlling rate, controlling stress and oscillation operating mode etc. The measurements carry through in a ZA15 sensor system, the system is a pair of the coaxial cylinders and the gap between the cylinders is 0.545 mm; the suspensions were placed into the gap, the intracylinder was stationary and the outer cylinder rotate at preconcerted rates while the apparatus was in working. The measured ranges are 0–3000 Pa for the stress and 0–300 s^{-1} for the shear rate. In this paper, the shear stresses and the viscosities of the samples were determined in different electric field strengths (E, DC field) at 25°C.

Because of the difficulty of directly measuring the dielectric properties of the particles, the suspensions of the materials were used to make dielectric investigation. The capacitance C and dielectric loss tangent ($\tan\delta$) at room temperature were obtained on a HP4274A Multi-frequency LCR Meter. The dielectric constant (ε) was derived from the measured C according to the conventional relation, $\varepsilon = C \cdot d/(\varepsilon_0 \cdot S)$, where ε_0 is the dielectric constant of vacuum i.e., 8.85×10^{-12} F m^{-1}, and d is the thickness of the gap between electrodes and S is the contact area of the electrodes.

3. Results and discussion

3.1. Crystal structure type and ER effect of the materials

The dependence of shear stress of ER suspensions of samples 1–8 on electric field strength at shear rate

Table 1
Compositions, crystal structures and grain size of particle materials

Sample no.	Calcination temperature (°C)	Composition	Grain sizes (nm)	Crystal structure
1	400	ZrO_2	8–10	Lattice: tetragonal; S.G: $P4_2/nmc$
2	400	$ZrO_2 + Y_2O_3$ (Zr:Y = 1:0.2 molar ratio)	4–5	Lattice: tetragonal; S.G: $P4_2/nmc$
3	400	$ZrO_2 + La_2O_3$ (Zr:La = 1:0.2 molar ratio)	4–5	Lattice: tetragonal; S.G: $P4_2/nmc$
4	400	$ZrO_2 + CeO_2$ (Zr:Ce = 1:0.2 molar ratio)	4–5	Lattice: tetragonal; S.G: $P4_2/nmc$
5	400	$ZrO_2 + Gd_2O_3$ (Zr:Gd = 1:0.2 molar ratio)	4–5	Lattice: tetragonal; S.G: $P4_2/nmc$
6	400	$ZrO_2 + Tb_2O_3$ (Zr:Tb = 1:0.2 molar ratio)	4–5	Lattice: tetragonal; S.G: $P4_2/nmc$
7	400	$ZrO_2 + ZrOCl_2$ (23: 1 molar ratio)	20–30	Lattice: tetragonal; S.G: $P4_2/nmc$ and lattice: monoclinic; S.G.: $P21/a$
8	600	ZrO_2	20–30	Lattice: monoclinic; S.G.: $P21/a$

$\gamma = 150\,s^{-1}$ was illustrated in Fig. 1, and the flow curves of samples 3, 4, 5 and 6 show that ER effects of these materials were very similar. In addition, in order to obtain a clear comparison of the ER performances of the eight types of materials, three types of viscosity were employed: the apparent viscosity of the suspension with and without applied electric field (η_E and η_0, respectively), and relative viscosity (η_r), which is defined in our work as the ratio of apparent viscosity to zero-field viscosity ($\eta_r = \eta_E/\eta_0$). Relative viscosity was also used to represent the magnitude of the ER activity. The corresponding data at $E = 4.2\,kV/mm$ and $\gamma = 150\,s^{-1}$ are listed in Table 2.

The results from both Fig. 1 and Table 2 show that the ER activity of sample 1 is much higher than that of sample 8, even though their compositions are the same. This can be explained by the difference in their crystal structure type. As is well known, XRD is the most important technique for the identification of ZrO_2 polymorphs; however, the broadening of the diffraction peaks arising from the small crystallite size effect makes it a little difficult to distinguish between the tetragonal and cubic symmetry [22]. Nevertheless, Raman spectra is an effective method for analyzing the crystal structure of fine particles, and many studies have focused on the Raman scattering of crystallite zirconia [23–26]. The

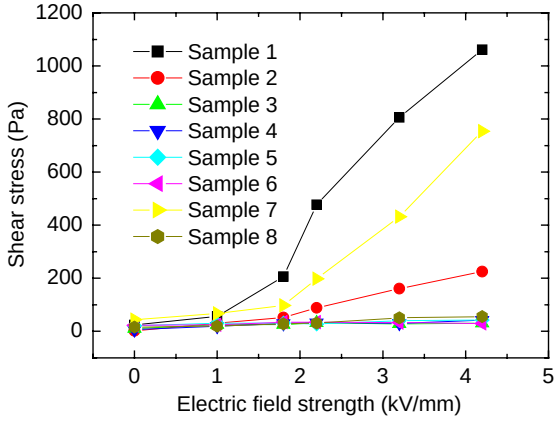

Fig. 1. Electric field strength dependence of shear stress of ER suspensions of samples 1–8.

Table 2
Relative viscosity of different materials at 25°C

Sample no.	η_0 (mPa s)	η_E (mPa s)	η_r
1	108.9	7068.0	64.9
2	66.97	1501.0	22.4
3	69.99	162.10	2.32
4	89.76	277.30	3.09
5	144.4	213.60	1.48
6	151.7	199.00	1.31
7	296.2	5024.0	17.0
8	102.1	403.50	3.95

Raman spectra of samples 1–6 and 8 were illustrated in Fig. 2. The results reveal that, the characteristic peaks of the cubic phase ZrO_2 do not appear [24]; the Raman spectra of samples 1–6 are similar; the bands at 269–273 cm^{-1}, 458–466 cm^{-1} and 630–642 cm^{-1} indicate that the crystal structures of the samples 1–6 all belong to tetragonal phase ZrO_2, and the bands at 292, 336, 380, 475, 538, 555, 620 and 633 cm^{-1} represent that the crystal structure of the sample 8 belongs to monoclinic phase ZrO_2 [24]. The Raman spectra of the sample 7 cannot be obtained due to the fluorescence arising from the existence of $ZrOCl_2$. Fig. 3 illustrated the XRD patterns of samples 1, 7 and 8. Both the Raman spectra and XRD patterns of the samples 1 and 8 show that, the ZrO_2 of the sample 1, which was obtained by decomposing the hydroxide of zirconium at 400°C, belongs to the tetragonal crystal system and space group $P4_2/nmc$; whereas the ZrO_2 of the sample 8, which was obtained by decomposing $ZrOCl_2$ at 600°C, is different from that of sample 1 to belong to the monoclinic crystal system

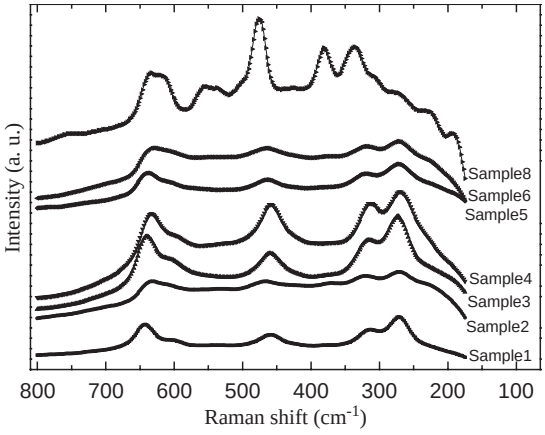

Fig. 2. Raman spectra of samples 1–6 and 8.

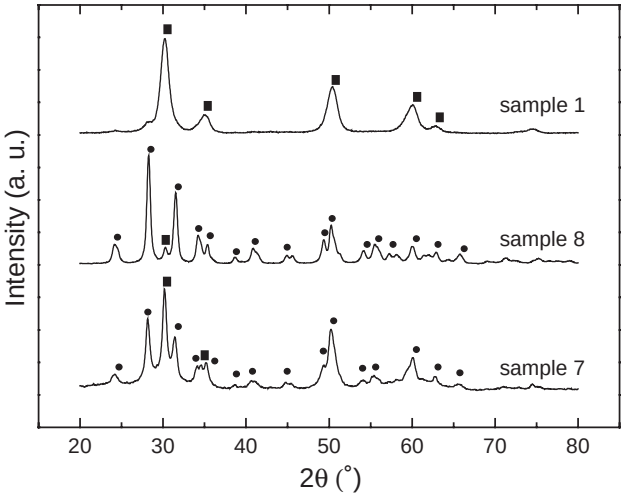

Fig. 3. XRD patterns of samples 1, 7 and 8 (■ tetragonal phase ZrO_2; • monoclinic phase ZrO_2).

and space group $P21/a$ (in the XRD patterns of sample 8, a very little peak appeared at 30.1° indicates only a little of the tetragonal phase ZrO_2 is contained in the monoclinic phase ZrO_2,). Furthermore, the ER activity of sample 7, which was obtained by decomposing $ZrOCl_2$ at 400°C, is better than that of monoclinic phase ZrO_2 (sample 8) and lower than that of tetragonal phase ZrO_2 (sample 1), which is related to its crystal structure type. Comparing the XRD patterns of sample 7 to those of samples 1 and 8, we could consider that the material of sample 7 consists of both the tetragonal phase and the monoclinic phase ZrO_2 (see Fig. 3). In the material of sample 7, the monoclinic content, referred to as f_m, can be obtained from XRD patterns using the following equation [22],

$$f_m = I_m(111)/[I_t(111) + I_m(111)],$$

where $I_t(111)$ and $I_m(111)$ are the intensities of the tetragonal phase and the monoclinic phase ZrO_2 at (111), respectively, the calculation result shows that the monoclinic content (84.5%) is more than that (15.5%) of the tetragonal phase. According to the ER performance of samples 1, 7 and 8 and their crystal structures, we can find that the ER activity of the material decreases with an increase of monoclinic phase ZrO_2. This result proves that the tetragonal phase ZrO_2 possesses higher ER activity than the monoclinic phase ZrO_2. The presence of small amount of $ZrOCl_2$ (ca 6%, weight%) in sample 7 may make its η_r value larger than that of sample 8, which has no $ZrOCl_2$, but less than that of sample 1. This shows that the influence of the change of structure type may be more important than that of a small amount of $ZrOCl_2$ on the ER effect of ZrO_2 material. The impact of $ZrOCl_2$ on the ER effect of ZrO_2 materials will be a subject of our future investigation.

The results in both Fig. 1 and Table 2 indicate that the ER activities of RE-doped ZrO_2 are all lower than that of ZrO_2 (sample 1), even though their crystal structures type is the similar (see Figs. 2 and 4, the small peaks of the La_2O_3 powder appears in the XRD pattern of sample 3, which may be due to separating out a little of La_2O_3 from the crystal lattice of ZrO_2 because the radii of the La^{3+} ion is the largest among the RE^{3+} ions). This is unusual in reported RE-doped materials. In order to find out the cause that leads to this unusual result, the surface area, pore volume, and pore diameters of sample 1 and samples of RE-doped ZrO_2 were measured on an ASAP 2010 Accelerated Surface Area and Porosimetry made by the US Micromeritics Company. The results revealed a distinct difference between the microstructures of sample 1 and RE-doped ZrO_2. The surface area of Y_2O_3–ZrO_2 (90.75 m^2/g) is larger than that of sample 1 (48.42 m^2/g); and the pore volume (0.0857 cm^3/g) and the average pore diameter (3.595 nm) of Y_2O_3–ZrO_2 are much smaller than those of sample 1 (0.267 cm^3/g and 21.14 nm). The corresponding data of other RE-doped ZrO_2 are in close approximation with those of Y_2O_3–ZrO_2. Therefore, it can be seen that doping rare earth oxide in ZrO_2 causes a decrease in the size of particles and a instantaneous increase in the surface area of the material; whereas at the same time it also causes decreases in the pore volume and the average pore diameter of the material. These changes in the microstructure, in particular, the decreases in the pore volume (the surface area of the pore, essentially) which would influence the interfacial polarization of a particle material in an electric field, can induce a fall in the ER activity of the material. It is, therefore, worthwhile to investigate further the interrelation between the material's ER effect and its crystal structural type and microstructure, as mentioned above, for ER particle materials.

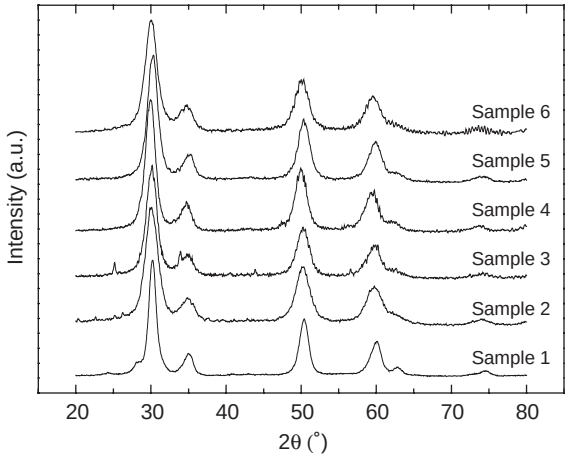

Fig. 4. XRD patterns of samples 1–6.

On the other hand, doping of RE oxides may cause a decrease in the number of oxygen atom defects in the ZrO_2 lattice, which leads to the decrease in the $\tan\delta$ value of the ZrO_2 particle material [27]. We also discovered that the ER activity of Y_2O_3–ZrO_2 is the strongest among all the RE-doped ZrO_2 materials. This fact may be accounted by the remarkable difference in the electron structure and ion radii, which may make the difference in the number of oxygen atom defects in the ZrO_2 lattice, between yttrium and lanthanide ions, the radii of Y^{3+} ion is the least among these RE^{3+} ions [28], and there is no f electron in the electron structure of Y^{3+} ion. As for the relation between the ER activity and the different rare earth ions, more work needs to be done in order to derive a more detailed mechanism.

3.2. Dielectric property and ER effect of the materials

The dielectric property of the materials at 2 kHz frequency indicates that the ε(3.13) and $\tan\delta$(0.025) values of the ER fluid of sample 1 are larger than the ε (2.72) and $\tan\delta$ (0.003) values of the Y_2O_3–ZrO_2 ER fluid. The ε and $\tan\delta$ values of other RE-doped ZrO_2

materials are very close to those of Y_2O_3–ZrO_2. Therefore, RE doping has caused a decrease in the ε and $\tan\delta$ values of the ZrO_2 ER fluid, and subsequently reduced the ER activity of RE-doped ZrO_2. The ε (2.98 and 1.65) and $\tan\delta$ (0.015 and 0.001) of both samples 7 and 8 are lower than that of sample 1. At any frequency in a range of 0.2–100 kHz, the trends that the ER effect changes with the change of the magnitude of the ε and $\tan\delta$ values are the same for different materials mentioned above, so, the case at 2 kHz frequency was selected as a representative. Tian Hao and his co-workers [29] proposed an empirical criterion for selecting ER material: the particle dielectric loss tangent should be approximately 0.10 at 1000 Hz, and the larger the particle dielectric constant, the stronger the ER effect. Therefore, above the correlation between dielectric property and ER effect is consistent with the empirical criterion obtained by Tian Hao et al.

3.3. Grain size and ER effect of the materials

In order to know further the relationship between the ER effect and the dispersion property of the material, the agglomerate degree of the particles in the materials were calculated, and the grain size of secondary particles of the materials were determined on Zeta Potential Analyzer (Type ZetaPlus) made by Brookhaven instruments Company (USA). From the following equation [30]

$$n = \frac{2d_x}{d_{N_2}}\left(1 - \frac{s}{s_t}\right), \quad s_t = \frac{6}{d_x \cdot Q_t},$$

where n is the number of the necks(an indication of the number of the grains per aggregate), d_x the grain diameter obtained from XRD line broadening measurements and d_{N_2} the diameter of a nitrogen molecule, s is the surface area attainable for the nitrogen molecules (the measured specific surface area), s_t is the theoretical surface area when it is assumed that each individual (spherical) grain can be completely covered with the nitrogen molecules, Q_t is the theoretical density of the material, the n values of the tetragonal phase ZrO_2 (sample 1), the RE-doped ZrO_2 and the monoclinic phase ZrO_2 (sample 8) were obtained as 23, 9–12 and 32, respectively, which show that the doping of the rare earth in ZrO_2 would lead to depress the agglomerate degree of the particle material. The grain sizes of secondary particles of samples 1, 4 and 8 were determined after dispersing the particle materials in the ethanol, respectively, and the distributions of the sizes were illustrated in Fig. 5. The results show that their size distributions are approximately 190–290 nm, 90–135 nm and 110–160 nm for samples 1, 4 and 8, respectively, which prove that there is still agglomerative phenomenon between the grains in the ethanol, but, the dispersion property in ethanol is better for the RE-doped ZrO_2 powders than for the pure ZrO_2 powders.

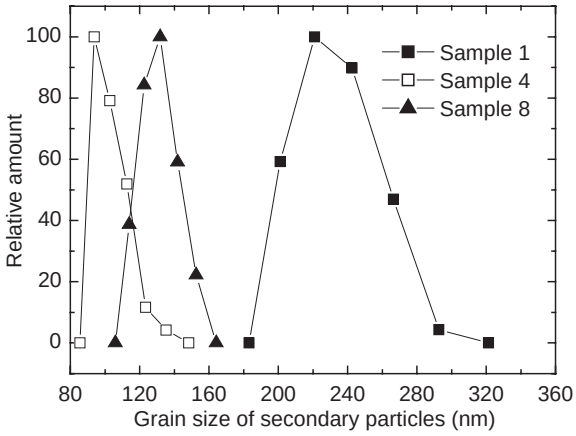

Fig. 5. Distributions of the grain size of secondary particles for samples 1, 4 and 8.

The average grain sizes of the particle materials were estimated by applying the XRD line broadening analysis using the Scherer formula [31], revealing a range of 5–30 nm. From Fig. 2, and the XRD patterns of Fig. 4 we can see that both pure ZrO_2 (sample 1) and RE-doped ZrO_2 (samples 2–6) powders belong to the tetragonal crystal system and space group $P4_2/nmc$; but the line widths of the XRD peaks are apparently larger for the RE-doped powders than for the pure ZrO_2 powders. This proves that the grain sizes (4–5 nm) of the RE-doped powders are smaller than those (8–10 nm) of the pure ZrO_2 powders. The similar results were displayed from the TEM micrographs of samples 1 and 4 (the grain sizes are approximately 8–15 nm and 5–8 nm, respectively), which were obtained on a JEM-200 CX electron microscope (see Fig. 6). Considering their ER activity mentioned above, such result indicates that when the grain sizes are too small, the ER performance of nano-sized particle materials can be played down by decreasing the particle sizes, since Brownian motion tends to compete with particle fibrillation [32]. However, the following experimental result was different from the case mentioned above. In Fig. 3, the line widths of the XRD peaks of samples 7 and 8 are smaller than those of sample 1. This proves that the grain sizes (20–30 nm) of ZrO_2 powders (samples 7 and 8, monoclinic phase) are larger than those of sample 1 powders (tetragonal ZrO_2); however, both ER activities are lower than that of sample 1. These facts indicate that both the crystal structure type and the grain sizes are important influencing factors for the ER performance of a nano-sized particle material, and the impact of the crystal structure type is dominant in both; but, the effect of particle sizes should be taken into account, too small grain sizes may be unfavorable for the ER effect, when the crystal structure types are the same and particle compositions are similar for the different nano-sized materials.

(a)

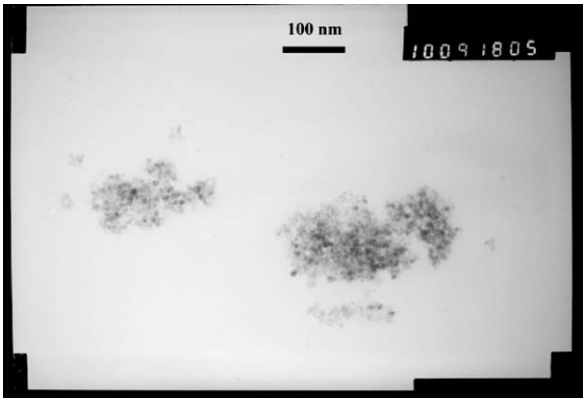

(b)

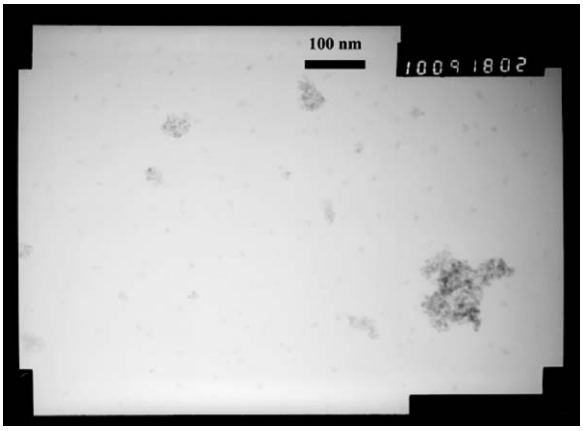

Fig. 6. TEM micrographs of samples 1 (a) and 4 (b).

From experimental results mentioned above, we find that doping the rare earth in ZrO_2 can reduce the grain size, the agglomerate degree and the grain size of secondary particles of the material. Therefore, the doping of the rare earth would change the surface property of a particle material, improve the dispersion property in a medium, which would influence the ER effect of a material.

4. Conclusion

Doping of rare earth oxide in ZrO_2 can reduce the ER activity of ZrO_2 material. The preparation method and calcination temperature can change the crystal structure type of a material. The polarity and dielectric property of the particles are related to their crystal structure type and other characteristics of the microstructure; therefore, the crystal structure is a very important factor in influencing the ER effect of a material. The ER activity of an ER material can be influenced by the grain sizes of the material for different materials in a system with identical crystal structure and similar composition.

Acknowledgments

We acknowledge support from the National Science Fund for Distinguished Young Scholars (20125104, 20221101), National Key Project for Fundamental Research (G1998061305).

References

[1] Z.P. Shulman, R.G. Gorodkin, E.V. Korobko, V.K. Gleb, J. Non-Newt. Fluid. Mech. 8 (1981) 29.
[2] T. Hao, Adv. Colloid Interface Sci. 97 (2002) 1.
[3] G.Y. Liu, Y.L. Zhang, X.M. Feng, J.K. Liang, G.H. Rao, J. Alloys Compd. 351 (1-2) (2003) 295.
[4] H. Bose, A. Trendler, Int. J. Modern Phys. B 16 (17–18) (2002) 2751.
[5] Y.L. Zhang, Y. Ma, J.K. Liang, G.G. Rao, K.Q. Lu, Mod. Phys. Lett. B 12 (4) (1998) 155.
[6] X.P. Zhao, J.B. Yin, L.Q. Xiang, Q. Zhao, Int. J. Mod. Phys. B 16 (17–18) (2002) 2371.
[7] X.P. Zhao, J.B. Yin, L.Q. Xiang, Q. Zhao, J. Mater. Sci. 37 (12) (2002) 2569.
[8] S.Z. Ma, J.R. Li, M.Y. Xu, S.X. Li, Acta Sci. Nat. Univ. Pekinensis 34 (4) (1998) 424 (in Chinese).
[9] X.P. Zhao, J.B. Yin, 2001 Chinese Patent No: 99115944.6.
[10] J.B. Yin, X.P. Zhao, Chin. Phys. Lett. 18 (8) (2001) 1144.
[11] M. Zhang, G.M. Qiu, C.H. Yan, Y.R. Li, J. Rare Earths 18 (4) (2000) 279.
[12] M.Y. Xu, S.Z. Ma, S.X. Li, J.R. Li, S.H. Zhang, S. Gao, J. Rare Earths 20 (6) (2002) 666.
[13] J.B. Yin, L.T. Guan, X.P. Zhao, Prog. Nat. Sci. 12 (4) (2002) 278.
[14] X.P. Zhao, J.B. Yin, Chem. Mater. 14 (5) (2002) 2258.
[15] J.B. Yin, X.P. Zhao, Chem. Mater. 14 (11) (2002) 4633.
[16] G.M. Qiu, L.X. Zhou, M. Zhang, Y.R. Li, C.H. Yan, J. Rare Earths 20 (1) (2002) 23.
[17] J.H. Park, Y.T. Lim, O.O. Park, Macromol. Rapid Commun. 22 (8) (2001) 616.
[18] Z.Y. Qiu, F.K. Shan, L.W. Zhou, F. Lu, Y.H. Zhu, Int. J. Mod. Phys. B. 15 (6–7) (2001) 618.
[19] W. Wen, W. Tam, P. Sheng, J. Mater. Res. 13 (1998) 2783.
[20] W. Tam, W. Wen, P. Sheng, Phys. B: Condens. Matter 279 (2000) 171.
[21] C.W. Wu, Y. Fahmy, H. Conrad, Int. J. Mod. Phys. B. 13 (14–16) (1999) 1775.
[22] E. Djurado, P. Bouvier, G. Lucazeau, J. Solid State Chem. 149 (2000) 399.
[23] K. Matsui, H. Suzuki, M. Ohgai, P. Arashi, J. Am. Ceram. Soc. 78 (1995) 146.
[24] C.M. Phillippi, K.S. Mazdiyasni, J. Am. Ceram. Soc. 54 (5) (1971) 254.
[25] V.G. Keramidas, W.B. White, J. Am. Ceram. Soc. 57 (1974) 22.
[26] M. Ishigame, T. Sakurai, J. Am. Ceram. Soc. 60 (1977) 367.
[27] V.M. Ferreira, J.L. Baptista, S. Kamba, J. Petzelt, J. Mater. Sci. 28 (1993) 5894.
[28] G.D. Zhou, Inorganic Structure Chemistry, Science Press, Beijing, China, 1984, p. 296.
[29] T. Hao, Z. Xu, Y. Xu, J. Colloid Interface Sci. 190 (1997) 334.
[30] W.F.M. Groot Zevert, A.J.A. Winnubst, G.S.A.M. Theunissen, A.J. Burggraaf, J. Mater. Sci. 25 (1990) 3449.
[31] A. Guiner, Theorie et Technique de la Radiocrystallographie, 3rd Edition, Dunod, Paris, France, 1964, p. 482.
[32] T. Hao, Adv. Mater. 13 (24) (2001) 1847.